Proceeding of the IEEE
International Conference on Robotics and Biomimetics
Dali, China, December 2019

Sensorless Power Assistance Control for a Lumbar Assist Device

Naoyuki Ogawa, Yusuke Ueta, Taiki Watanabe, Tsuyoshi Kaneko,
Peirang Li, Chang Liu, Hongbo Liang, Naoya Ueda and Chi Zhu
Department of Systems Life Engineering
Maebashi Institute of Technology
460-1, Kamisadori, Maebashi, Gunma, Japan
{m1856006, zhu}@maebashi-it.ac.jp

Weimin Zhang
Beijing Institute of Technology
5 South Zhongguancun Street, Haidian District, Beijing, China

Yasuyuki Shibusawa, Naoki Tago and Koei Deguchi
YAMADA MANUFACTURING CO.,LTD.
2-1296, Kobayashi, Isesaki, Gunma, Japan

***Abstract*— This paper presents a sensorless control for human's lumbar power assistance by our developed lumbar assist device (LAD). The proposed sensorless control is realized by a disturbance observer and an extended admittance model. The disturbance observer is developed to estimate the torque that the wearer applies to the lumbar assist device, and the extended admittance model is adopted to generate the target angular velocity of the lumbar assist device. The power assistance experiments with our LAD are conducted. The effect of the power assistance evaluated by EMG signal and heart rate shows that the wearer's burden is decreased by about 8% and 10%, respectively. These results show that the proposed sensorless control for lumbar power assistance is effective.**

***Index Terms*— power assistance, sensorless control, disturbance observer, lumbar assist device**

I. Introduction

Recently in many advanced countries, the aging population is increasing, and the birth rate is decreasing. Due to the aging of society and shrinking of production ages, the elderly taking care of the elderly and labor shortage have become serious problems. To alleviate this social problem, development of wearable powered exoskeleton robot suits to reduce the human burden has increased in these two decades. In such developed wearable powered exoskeleton robot suits, electromyography (EMG) or force/torque sensors are widely used for control purposes.

The robot suit HAL developed by Cyberdyne Inc. and the assistive device developed by Kiguchi et al are the examples. HAL lumbar type is able to assist the wearer naturally by the EMG signals from the back as control signal [1]. The assistive device developed by the Kiguchi et al is able to implement the precise moment with total of 7 degrees of freedom, in which 3 degrees of freedom on the shoulder, 1 degree freedom of elbows, and 2 degrees of freedom on the wrist by using 16 EMG sensors on the upper limb [2] [3]. The biggest merit using EMG signals is that measurement of the biosignal is possible and can assist the wearer in real time [4]. However, since there need more EMG sensors to detect the wearer's movement from biarticular muscles, there exist some problems. For example, it takes time to attach EMG electrodes at the right places; dealing with the variation of the signal from individual differences are difficult; and the sensors are easy to peel off from the wearer's skin due to sweat and movement.

On the other hand, the force/torque sensors are used in EXO-UL7 developed by Jacob et al and Curara developed by the AssistMotion Inc. EXO-UL7 can control a 7 DoF of upper limb by a force sensor attached on the tip of the hand [5], while Curara uses torque sensors attached to each joint to control its movements [6] [7]. With force/torque sensors, there is no need to attach the other sensors on the wearer's body and the force/torque sensor signal is more stable than the biosignal signals like EMGs. However, the number of sensors increases with the number of assisting joints and the cost will be increasing too.

Meanwhile, there are some studies on force sensorless control, in which the external force of the robot is estimated by disturbance observer and therefore the expensive force/torque sensors are not required. The disturbance observer is used for the identification of robot's dynamics, sensorless motion control on electric wheelchair, and so on [8] [9] [10] [11].

In this study, we develop a sensorless control system for human's lumbar power assist by our developed lumbar assist device (LAD). This system consists of a torque estimation model and an extended admittance model. The torque estimation model, which in fact is a disturbance observer, is for estimating the torque applied by the wearer to the lumbar assist device. The extended admittance model, that is proposed in our previous research, is used to generate the target angular velocity of the LAD based on the estimated

978-1-7281-6321-5/19//$31.00 ©2019 IEEE

torque. With a simple PID control the power assistance for lumbar is realized and the effectiveness of the proposed approach is confirmed.

II. The overview of the developed lumbar power assist device

In this study, we construct a sensorless control system for the lumbar power assist device that is being developed in our laboratory. As shown in Fig.1. The power assist device is designed a backpack typed that is carried by a shoulder belt and fixed to the waist by the belt near the center of rotation. In addition, its two identical drive units are symmetrically located on the left and right waist respectively and their output parts are fixed to the wearer's left and right thighs by the belts. Fig.2 shows the structure of the driving unit of the lumber power assist device. The power of the brushless DC motor is transmitted to the output axis through the first pulley, timing belt, second pulley, and reduction gear. The total reduction ratio from the motor to the output axis is 39, and the efficiency from the motor to the output axis was determined to about 73.5%.

Fig. 1. A under developed lumbar power assist device

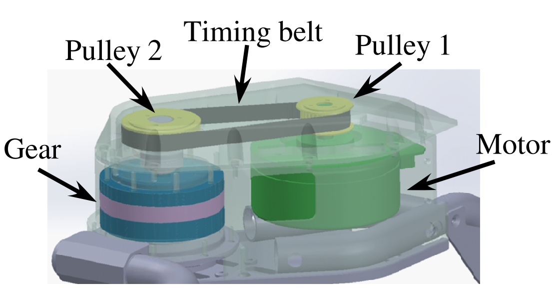

Fig. 2. Structure of the driving unit of the lumber power assist device

III. Torque estimation by disturbance observer

A. Model of Brushless Direct Current Motor

The motion equation of a brushless DC motor used in our lumbar assist device (LAD) is expressed as

$$J_M \frac{d\omega_M}{dt} + T_l = K_t i_{ref} \tag{1}$$

where J_M is the moment of inertia of the motor, ω_M is the angular velocity of the motor, T_l is the load torque, K_t is the torque constant of the motor, and i_{ref} is the motor's command armature current. Eq.(1) can be further reformulated as Eq.(2), which in fact, is a disturbance observer of the brushless DC motor

$$\hat{T}_{dis} = K_{tn} i_{ref} - J_{Mn} \frac{d\omega_M}{dt} \tag{2}$$

where, $\hat{T}_{dis}$ is the disturbance torque of the motor and the subscripts n represents the nominal values of the torque coefficient and moment of inertia. The block diagram of Eq.(1) and Eq.(2) are illustrated in dotted line block shown in Fig. 3, respectively. The disturbance torque can be estimated by this model. From the estimated disturbance torque, a compensation current i_{cmp} is calculated and a robust control system is constructed by feedback of this current to the motor.

B. Components of Disturbance Torque

In the subsection III-A, the disturbance torque model of the brushless DC motor is constructed, but there are many kinds of disturbances acting on the joints of the robot. Here, we discuss the components of the disturbance torque T_{dis} on robot joint. The summation of the disturbances can be expressed as

$$\begin{aligned} T_{dis} = T_{int} + T_g + T_{ext} + T_f + D\omega_M \\ +(J_M - J_{Mn})\frac{d\omega_M}{dt} + (K_{tn} - K_t) i_{ref} \end{aligned} \tag{3}$$

where, T_{int} is the interference torque from other joints, T_g is the torque due to gravity, T_{ext} is the reaction torque from

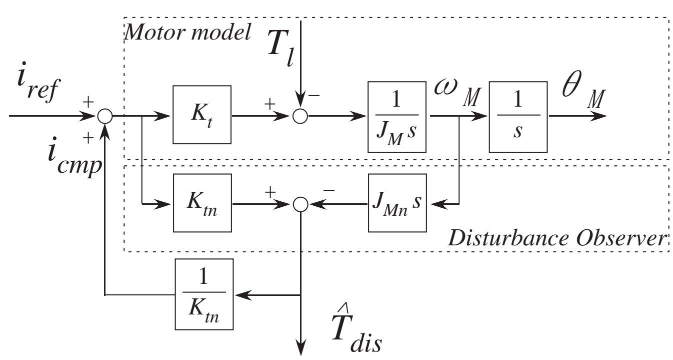

Fig. 3. A DC motor model and its disturbance observer

the external of the robot, $T_f + D\omega_M$ are the friction torques from reduction gears and motor, $(J_M - J_{Mn})\frac{d\omega_M}{dt}$ is the fluctuation of moment of inertia, and $(K_{tn} - K_t)i_{ref}$ is the torque ripple.

C. Estimation of Reaction Torque

The wearer's applied force/torque to LAD is the control signal of the device. Since the reaction torque is generated when the wearer tries to move the LAD to perform a task, a reaction torque model is necessary to estimate the wearer's torque. Assuming that the torque ripple of motor is so smaller that it could be neglected, and the other torques such as the interference torque from other joints, the torque due to gravity, the frictional torque, the fluctuation torque of moment of inertia are identified from experiment in advance, the reaction torque $\hat{T}_{ext}$ can be estimated as shown in Fig. 4.

1) Dynamics model of the robot: The length, weight, moment of inertia and other parameters of each link are needed for the dynamics model of the robot. Since the lumbar assist device assists in flexion and extension direction of lumbar, we model the lumbar assist device as a 2 DoF manipulator as shown in Fig. 5. Considering the link's center position of gravity, let the i-th link's center position of gravity be (x_{gi}, y_{gi}), the distance between (x_{gi}, y_{gi}) and i-th joint be l_{gi}, the mass of i-th link be m_i, the moment of inertia of i-th link be I_i, gravitational acceleration be g[m/s^2], and the

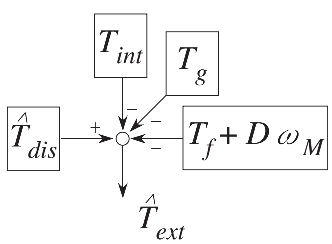

Fig. 4. Estimation of Reaction torque

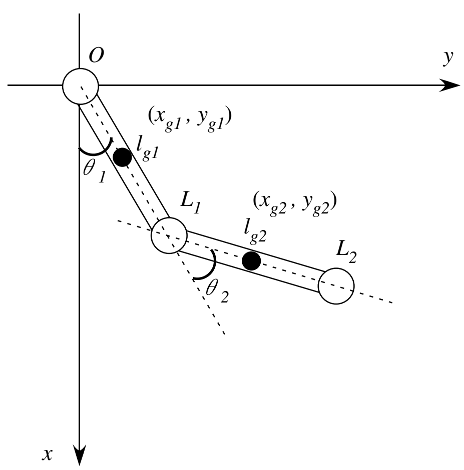

Fig. 5. Two DoF manipulator

torque of i-th motor be τ_i[Nm]. The dynamic equation of the robot can be expressed as

$$M(\boldsymbol{\theta})\ddot{\boldsymbol{\theta}} + \boldsymbol{h}\left(\boldsymbol{\theta}, \dot{\boldsymbol{\theta}}\right) + \boldsymbol{g}(\boldsymbol{\theta}) = \boldsymbol{\tau} \tag{4}$$

$$M(\boldsymbol{\theta}) = \begin{bmatrix} A_{11} & A_{12} \\ A_{21} & A_{22} \end{bmatrix} \tag{5}$$

$$A_{11} = m_1 l_{g1}^2 + m_2 l_1^2 + m_2 l_{g2}^2 + I_1 + I_2 + 2m_2 l_1 l_{g2}\cos\theta_2$$
$$A_{12} = m_2 l_{g2}^2 + I_2 + m_2 l_1 l_{g2}\cos\theta_2$$
$$A_{21} = m_2 l_{g2}^2 + I_2 + m_2 l_1 l_{g2}\cos\theta_2$$
$$A_{22} = m_2 l_{g2}^2 + I_2$$

$$\boldsymbol{h}\left(\boldsymbol{\theta}, \dot{\boldsymbol{\theta}}\right) = \begin{bmatrix} -m_2 l_1 l_{g2}\left(2\dot{\theta}_1 + \dot{\theta}_2\right)\dot{\theta}_2\sin\theta_2 \\ m_2 l_1 l_{g2}\dot{\theta}_1^2\sin\theta_2 \end{bmatrix} \tag{6}$$

$$\boldsymbol{g}(\boldsymbol{\theta}) = \begin{bmatrix} (m_1 g l_{g1} + m_2 g l_1)\cos\theta_1 + m_2 g l_{g2}\cos(\theta_1 + \theta_2) \\ m_2 g l_{g2}\cos(\theta_1 + \theta_2) \end{bmatrix} \tag{7}$$

where $\boldsymbol{\tau} = \begin{bmatrix} \tau_1 & \tau_2 \end{bmatrix}^{\mathrm{T}}$, and $\boldsymbol{\theta} = \begin{bmatrix} \theta_1 & \theta_2 \end{bmatrix}^{\mathrm{T}}$. From Eq. (4) to (7), the interference torques from the other joints, torques due to gravity, and the fluctuation torque of moment of inertia can be obtained.

2) Identification of Frictional Torques: We conducted experiments to identify the frictional torques existing in the motor and the gears. When there is no load in the output axis of the reduction gears and the motor rotates at a constant speed, the influences of gravity and the moment of inertia can be neglected, only frictional torque is acting on the system. In order to create the above state, the experiment is conducted as shown in Fig 6. In this case, the motor's driving torque is equal to the frictional torques which is expressed as

$$K_t i_{ref} = T_f + D\omega_M. \tag{8}$$

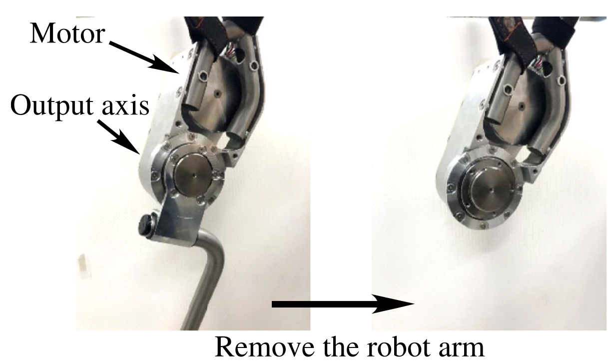

Fig. 6. Identification of Frictional Torques

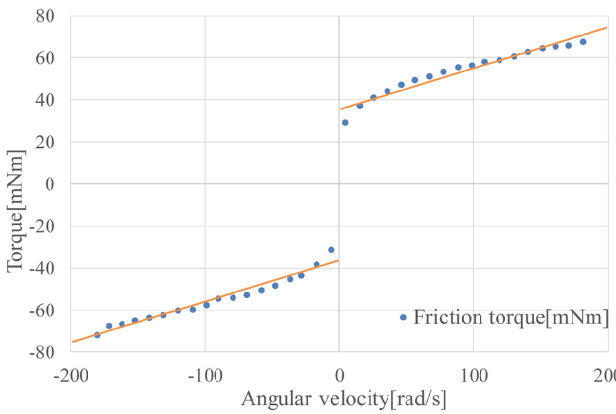

Fig. 7. Result of frictional torque

In the experiment, the current value for each angular velocity is recorded, and the friction torque is obtained from Eq. (8). The results of the frictional torque are shown in Fig. 7. The estimated frictional torques are shown in dotted line and its linear approximation obtained by the least square method is shown in orange solid line. The linear approximation is expressed as

$$T_f + D\omega_M = a + b\,\omega_M, \quad as\ \omega_M < 0 \tag{9}$$

$$T_f + D\omega_M = c + d\,\omega_M, \quad as\ \omega_M > 0 \tag{10}$$

where $a = -37.0$, $b = 0.192$, $c = 36.4$, and $d = 0.187$.

IV. SENSORLESS CONTROL FOR POWER ASSISTANCE

With the estimated torque, sensorress power assistance control is constructed and the power assistance experiments to support the flexion and extension movement of the wearer's lumbar joint are conducted.

A. Torque estimation of lumbar joint

With the above results, estimation of the torque of lumbar joint is conducted. As shown in Fig. 8, a force sensor is attached at the tip of output part of our lumbar power assist device to verify the estimated torque. In the experiments, we exert a pull force on the force sensor and flex the joint from 0° to 90°. The experiments are conducted three times, and the results are shown in Fig. 9. The results show that the estimated torque and the measured torque calculated from the measured force coincide very well. Hence, the effectiveness of the estimation approach is verified.

B. Extended admittance model and its based control

The estimated torque of the wearer applied to the LAD is the input of our proposed extended admittance model that is proposed in our previous study [11] [12] [13]. The extended admittance model generates the target angular velocity of the LAD joint from the estimated torque, and then its angular velocity is controlled by a simple PID control. The diagram of the whole control block is shown in Fig.10.

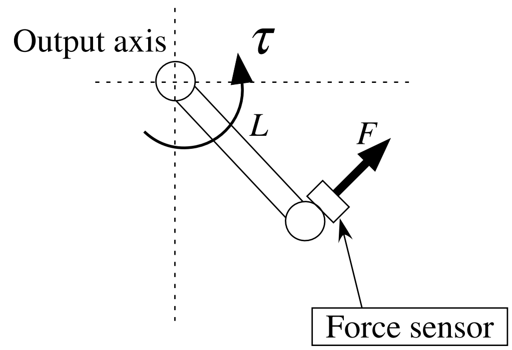

Fig. 8. Experiment method of torque estimation

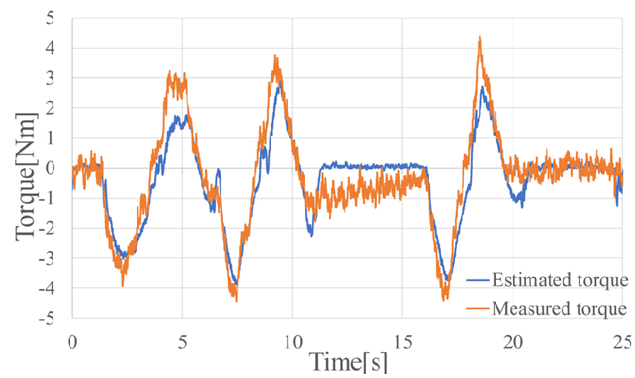

Fig. 9. Comparison of the estimated torque and the measured torque from force sensor

The extended admittance model is expressed in Eq.(11) and shown in Fig. 11.

$$\tau_h - \tau_0 = I\dot{\omega}_d + D\omega_d \tag{11}$$

where τ_h is the input torque of which the wearer applied to the robot; I and D are the virtual moment of inertia and the virtual coefficient of damping, respectively, which can be arbitrarily set in advance; τ_0 represents the wearer's necessary joint torque to keep the load. By having been changed I, the responses of the robot would be also changed. Moreover, by changing D, the assist ratio is changed, and it is possible to adjust the load feeling of the wearer.

There are three movement modes of the LAD as follows:

- flexion mode, $\omega_d > 0$, as $\tau_h > \tau_0$
- keeping mode, $\omega_d = 0$, as $\tau_h < \tau_0$
- extension mode, $\omega_d < 0$, as $\tau_h < \tau_0$

This extended admittance control can seamlessly realize the switching of the three control modes and it is verified in [11] [12] [13].

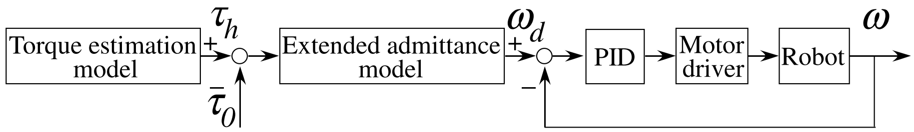

Fig. 10. The control block of our proposed sensorless power assistance

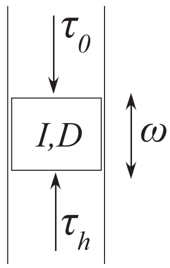

Fig. 11. Extended admittance model

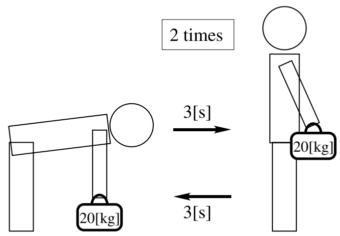

Fig. 12. Power assistance experiments evaluated by EMG signals

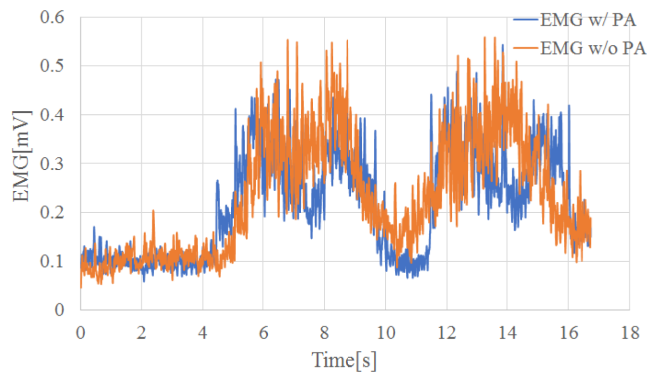

Fig. 13. Result comparison with PA and without PA evaluated by EMG

TABLE I

EMG Comparison with and without PA

	EMG(w/o PA)[mV]	EMG(w/ PA)[mV]
Subject A	0.30	0.27
Subject B	0.40	0.37
Subject C	0.28	0.26

C. Evaluation by EMG

The experiments of power assistance for wearer's lumbar joint are implemented using the developed sensorless control approach.

1) Method of evaluation by EMG: The experimental method is shown in Fig. 12. Subjects were 3 males in their 20s. The subject wears the LAD and holding 20[kg] load. The task is that the wearer first flexes his lumbar joint from 0°to 90° and keep it in rest, then extends his lumbar joint from 90° to 0°. In the experiments, we simultaneously measure the EMG signals of the erector spine muscles. The experiments are performed two times.

2) Results of evaluation by EMG: The experiment results are shown in Table I. As an example, subject A's experiment results are shown in Fig. 13. From the results of Table I, the average of EMGs of three subjects without power assistance (PA) is about 0.32 [mV], while the average of EMGs with PA is about 0.30 [mV].

The decreased average of EMGs is about 8%. This implies that the wearer's burden is reduced by about 8%.

There are two possible reasons why the decrease in EMGs remained only about 8%. The first is that the lumbar assist device is heavy, about 10 [kg]. Since the weight of the LAD is directly applied to the wearer through the shoulder and waist belt, though the wearer feels large assist force from the LAD via the shoulder belts, there is a possibility that the weight of the LAD counteracts the power assist effect of LAD, because the erector spine muscles have to endure the weight of LAD and the load simultaneously. The second point is the human's muscle can't exert its contracting force when the joint reaches its bending limit or the muscle extends full extension [14]. In this regard, it has been reported that the EMG corresponding to a load caused by bending cannot be obtained in a forward bending posture with a large angle [15]. In our experiments, the subject's bending angle is large at approximately 90°, consequently, the EMG signals corresponding to the load may not be obtained. In future experiments, it will be necessary to examine the flexion and extension angle.

D. Evaluation by heart rate

1) Method of evaluation by heart rate: In this subsection, in order to further verify the effect of the power assist of our LAD, the exercise intensity is evaluated with the subject's heart rate. It has been shown that there is a strong correlation among heart rate, exercise intensity, and energy consumption from previous study [16] [17]. Here, we use the exercise intensity to evaluate the load during the movement, or saying, exercise. Eq. (12) shows how to calculate exercise intensity (EI).

$$EI = \frac{HR - HR_{rest}}{HR_{max} - HR_{rest}} \times 100 \tag{12}$$

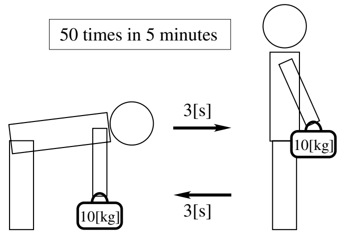

Fig. 14. Power assistance experiments evaluated by heart rate

TABLE II
HEART RATE(HR) COMPARISON WITH AND WITHOUT PA

		Resting	w/o PA	w/ PA
Subject A age:24	HR[bpm]	62	81	67
	EI[%]	0	14.2	3.7
Subject B age:22	HR[bpm]	79	110	96
	EI[%]	0	26.1	14.3
Subject C age:21	HR[bpm]	66	80	70
	EI[%]	0	10.5	3.0

where, HR is the measured heart rate, HR_{rest} is the heart rate at rest, and HR_{max} is the maximum heart rate. The maximum heart rate can be generally calculated from the age of the subject as shown in Eq. (13) [18].

$$HR_{max} = 220 - age \tag{13}$$

2) Results of evaluation by heart rate: The state of the experiment is shown in Fig. 14. Subjects were 3 males in their 20s. He flexes his lumbar joint in 3 seconds and then extends his lumbar joint in 3 seconds. These movements are taken as one set, and the subject performs 50 sets in 5 minutes. The above tasks are conducted with and without PA, respectively, and his heart rate are measured immediately after finishing the task. Table II shows the measurement results of the three subjects.

From the results of Table II, the average of EI of three subjects without PA is 16.9%, and the EI with PA is 7.0%.

Therefore, the exercise intensity is greatly decreased under the power assist of our developed LAD.

V. CONCLUSION

In this paper, a sensorless control for human's lumbar power assistance by our developed lumbar assist device (LAD) is proposed and examined. This control is constructed by a disturbance observer and an extended admittance model. The disturbance observer is for estimating the torque that the wearer applies to the LAD, and the extended admittance model is used to generate the target angular velocity of the LAD from the estimated wearer's torque. The experimental results evaluated by EMG signals show that the wearer's burden is decreased by about 8%. The reason of this small value is discussed. Further, the experimental result evaluated by heart rate shows the load on the wearer has been decreased by 10%. The effectiveness of the power assistance of the lumbar assist device is verified, and hence the proposed sensorless power assistance control is successfully realized.

REFERENCES

[1] Hiromasa Hara, Yoshiyuki Sankai, Development of HAL for Lumbar Support, SCIS & ISIS 2010, TH-D4-2, Dec 2010.
[2] Ranathunga Arachchilage Ruwan Chandra Gopura, Kazuo Kiguchi, Mechanism and Control of a 7DOF Upper-Limb Power-Assist Robot, JSME annual meeting, pp.345-346, 2009.
[3] K.Kiguchi and Y.Hayashi, An EMG-based control for an upper-limb power-assist exoskeleton robot, IEEE TRANSACTIONS ON SYSTEMS, MAN, AND CYBERNETICS-PART B: CYBERNETICS, VOL. 42, NO. 4, AUGUST 2012.
[4] AGNIESZKA SZPALA, ALICJA RUTKOWSKA-KUCHARSKA, MATEUSZ STAWIANY, Symmetry of electromechanical delay, peak torque and rate of force development in knee flexors and extensors in female and male subjects, Acta of Bioengineering and Biomechanics, vol.17, No.1, 2015.
[5] Wen Yu, Jacob Rosen and Xiaoou Li, PID Admittance Control for an Upper Limb Exoskeleton, Proceedings of American Control Conference (ACC), pp.1124-1129,2011.
[6] AssistMotion Inc., About curara®, http://assistmotion.jp/, accessed on 20 September 2019.
[7] Atsushi Tsukahara, et al., Evaluation of walking smoothness using wearable robotic system curara for spinocerebellar degeneration patients, Proceedings of 2017 International Conference on Rehabilitation Robotics (ICORR), July 17-20, pp.1494-1499, 2017.
[8] Toshiyuki MURAKAMI and Kouhei OHNISHI, Dynamics Identification Method of Multi-Degrees-of-Freedom Robot Based on Disturbance Observer, Journal of the Robotics Society of Japan, Vol.11, No.1, pp.131-139, 1993.
[9] Toshiyuki Murakami, Fangming Yu and Kouhei Ohnishi, Torque sensorless control in multidegree-of-freedom manipulator, IEEE TRANSACTIONS ON INDUSTRIAL ELECTRONICS, VOL. 40, NO. 2, APRIL 1993.
[10] Sehoon Oh and Yoichi Hori, Sensor Free Power Assisting Control Based on Velocity Control and Disturbance Observer, Proceedings of the IEEE International Symposium on Industrial Electronics, pp.1709-1714, 2005.
[11] C.Zhu, et al., Power augmentation of upper extremity by using agonist electromyography signals only for extended admittance control, IEEE Journal of Industry Applications, Vol.3 No.3 pp.260-269,2014.
[12] C.Liu, et al., Development of a light wearable exoskeleton for upper extremity augmentation, Proceedings of the 23rd International Conference on Mechatronics and Machine Vision in Practice (M2VIP), Nanjing, China, 28-30 Nov. 2016.
[13] C.Zhu, Shota Shimazu, Masataka Yoshioka and Tomohiro Nishikawa, Power assistance for human elbow motion support using minimal EMG signals with admittance control, Proceedings of the 2011 IEEE International Conference on Mechatronics and Automation August 7 - 10, Beijing, China.
[14] Akihiko SEO, Hiroshi UDO, and Fumitaka YOSHINAGA, Electromyogram measuring method for low back load evaluation of handling weight and forward bending posture, Japanese journal of industrial health, 35, 19-24, 1993.
[15] Floyd WF, Silver PHS, The function of the erectores spinae muscles in certain movements and postures in man, J Physiol, 129, 184-203, 1955.
[16] Akihiko Tajima, Assessment of energy expenditure: an association between heart rate and oxygen uptake in daily physical activity, International journal of analytical bio-science 2(4), 135-142, 2014-12.
[17] Goldsmith R, Miller DS, Mumford P, et al.: The use of long-term measurements of heart rate to assess energy expenditure. J Physiol, 189(2): 61-62, 1967.
[18] American College of Sports Medicine. ACSM's guidelines for exercise testing and prescription. Philadelphia, PA: Lippincott Williams & Wilkins, CHAPTER7 Methods of Estimating Intensity of Exercise, 2007.